



Universiteit  
Leiden  
The Netherlands

## "Skipping orbits traversing trajectories; quantum ballistic transport in microstructures"

Beenakker, C.W.J.; Houten, H. van; Wees, B.J. van

### Citation

Beenakker, C. W. J., Houten, H. van, & Wees, B. J. van. (1989). "Skipping orbits traversing trajectories; quantum ballistic transport in microstructures". Retrieved from <https://hdl.handle.net/1887/3329>

Version: Not Applicable (or Unknown)  
License: [Leiden University Non-exclusive license](#)  
Downloaded from: <https://hdl.handle.net/1887/3329>

**Note:** To cite this publication please use the final published version (if applicable).

## SKIPPING ORBITS, TRAVERSING TRAJECTORIES, AND QUANTUM BALLISTIC TRANSPORT IN MICROSTRUCTURES

C.W.J. Beenakker and H. van Houten<sup>a</sup>

Philips Research Laboratories, 5600 JA Eindhoven, The Netherlands

B.J. van Wees

Department of Applied Physics, Delft University of Technology  
2600 GA Delft, The Netherlands

(Received 8 August 1988)

Three topics of current interest in the study of quantum ballistic transport in a two-dimensional electron gas are discussed, with an emphasis on correspondences between classical trajectories and quantum states in the various experimental geometries. We consider the quantized conductance of point contacts, the quenching of the Hall effect in narrow channels, and coherent electron focusing in a double-point contact geometry.

### 1. Introduction

Quantum ballistic transport in a two-dimensional electron gas (2DEG) is a fascinating new field of research, enabled by advances in molecular beam epitaxy and microfabrication techniques. On the one hand, GaAs-AlGaAs heterostructures can be grown which have very little impurity scattering in the 2DEG, so that large mean free paths, on the order of 10  $\mu\text{m}$ , are realized. Motion of the electrons on this length scale proceeds along ballistic trajectories involving repeated collisions with the boundary. On the other hand, it has become possible to fabricate microstructures with minimal dimensions comparable to the De Broglie wave length  $\lambda_F \sim 50$  nm of the current-carrying electrons at the Fermi level. On this length scale the interference of electrons moving on different trajectories leads to interesting quantum phenomena. Three recently discovered examples are reviewed in this article.

Our discussion is in terms of two alternative ways of treating quantum ballistic transport through a 2DEG channel: Either in terms of interfering trajectories (as in a Feynman path integral), or in terms of a discrete set of quantum states or 1D subbands. These two equivalent ways of description are analogous to the ray *versus* mode description of propagation through an optical fiber or wave guide. We have found this analogy with optics fruitful, both to understand the experiments and to inspire new ones. In the semi-classical approximation only interferences of classical trajectories are retained. This is equivalent

to solving the Schrödinger equation in the WKB approximation. The quantum states are then simply given by the Bohr-Sommerfeld quantization rule. The character of the quantum states can be continuously changed by applying an external magnetic field, oriented perpendicular to the 2DEG. We will discuss a "phase diagram", in which the quantum states (and the corresponding trajectories) are classified according to their lateral extension in edge states (skipping orbits), traversing states, and Landau levels (cyclotron orbits). We believe that many essential features of quantum ballistic transport can be understood on the basis of this simple classification.

The three examples considered all involve transport through microstructures defined in the 2DEG of a GaAs-AlGaAs heterostructure. We first consider point contacts, in section 2. The residual resistance in the ballistic transport regime of a short and narrow channel connecting two broad regions (a point contact) is due to electrons which are reflected at the channel entrance. In metals, this resistance is known as the Sharvin contact resistance<sup>1</sup>, and can be described classically since there  $\lambda_F \sim 0.5$  nm is much smaller than achievable point contact widths. In the 2DEG, however,  $\lambda_F$  is a hundred times as large, a length scale which is within reach of lithographical techniques. This has enabled our group<sup>2</sup>, and independently a group from the Cavendish laboratory<sup>3</sup>, to fabricate a quantum point contact (QPC) of variable width comparable to  $\lambda_F$ . We discuss the origin of the conductance quantization in a QPC in terms of the analogy with an electron wave guide<sup>4</sup>. In section 3 we consider the correspondences between quantum states and classical trajectories in a narrow 2DEG channel in a weak magnetic field, and discuss a possible theoretical explanation<sup>5</sup> for the quenching of the

a. Present address: Philips Laboratories, Briarcliff Manor, NY 10510, USA.

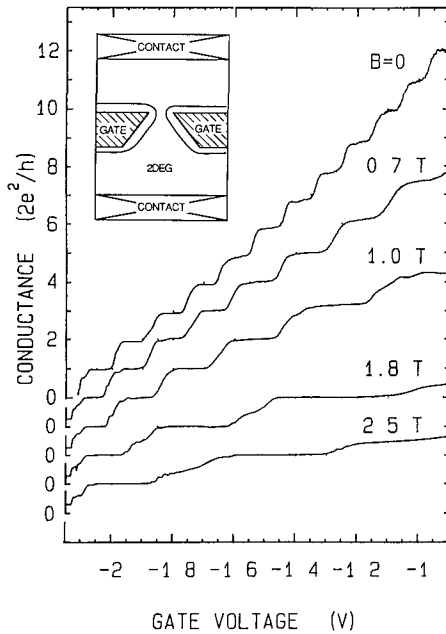


**Fig. 1.** Point contact conductance (corrected for a series lead resistance) as a function of gate voltage for several magnetic field values, illustrating the transition from zero-field quantization to quantum Hall effect. The curves have been offset for clarity. The inset shows the device geometry, with the depletion regions defining the point contact indicated schematically. (Fig. taken from Ref. 2.)

Hall effect discovered experimentally by Roukes *et al.*<sup>6</sup>. Finally, in section 4, we consider coherent electron focusing<sup>7</sup> (CEF) in a geometry involving two adjacent point contacts on a single boundary of the 2DEG. This experiment allows one to study the interference of skipping orbits along the 2DEG boundary<sup>8</sup>. From a different point of view, CEF is a typical example of a non-local voltage measurement, which provides a demonstration of the reciprocity relation for non-local phase-coherent transport derived by Büttiker<sup>9</sup>.

## 2. Quantum point contacts

The QPC is a narrow and short channel of variable width  $W \sim \lambda_F \sim 50$  nm, defined in the 2DEG by applying a negative voltage on a split gate on top of the heterostructure (see Fig. 1, inset). The channel length  $L \gtrsim W$  is much smaller than the mean free path  $l \sim 10 \mu\text{m}$ . As discovered recently<sup>2,3</sup>, the contact conductance  $G_c$  of a QPC is approximately quantized in units of  $2e^2/h$ , *without a magnetic field*. If a magnetic field is applied perpendicular to the 2DEG, a continuous transition to the quantum Hall effect is observed (Fig. 1). Additional plateaus at odd multiples of  $e^2/h$  are resolved above fields of about 2 T, as

the magnetic field removes the spin degeneracy. [These additional plateaus are also resolved in parallel fields<sup>3</sup>, but much higher fields exceeding 10 T are required; This may be due to the anisotropic enhancement of the Landé  $g$ -factor in quasi 1D channels found by Smith *et al.*<sup>10</sup>.] In Ref. 2 we gave a semiclassical explanation<sup>11</sup> of the zero-field quantization, based on the assumption of quantized transverse momentum in the QPC, and discussed the fundamental relation between contact resistances and Landauer's formula<sup>12</sup> which was pointed out by Imry<sup>13</sup>.

**Table 1.** The electron wave guide

ray	$\Leftrightarrow$	trajectory
mode	$\Leftrightarrow$	subband
mode index	$\Leftrightarrow$	quantum number $n$
wave number $k$	$\Leftrightarrow$	canonical momentum $\hbar k$
frequency $\omega$	$\Leftrightarrow$	energy $\varepsilon = \hbar\omega$
dispersion law $\omega(k)$	$\Leftrightarrow$	band structure $\varepsilon_n(k)$
group velocity $d\omega/dk$	$\Leftrightarrow$	velocity $d\varepsilon/\hbar dk$

In terms of the wave guide analogy (Table 1), the conductance quantization arises because *the current is shared equally among an integer number of excited modes*, despite the fact that different modes  $n=1,2,\dots,N$  have different group velocities  $v_n = d\varepsilon_n/\hbar dk$ . The point is that the group velocity cancels with the density of states  $\rho_n = (\pi d\varepsilon_n/dk)^{-1}$  (both evaluated at the Fermi energy), so that the current per mode is  $e v_n \rho_n eV = (2e^2/h)V$  – regardless of energy or mode index. The conductance, which is the total current divided by the applied voltage  $V$ , then becomes

$$G_c = N \frac{2e^2}{h}, \quad (1)$$

as observed experimentally<sup>2,3</sup>.

For an infinite barrier confining potential,  $N$  is the largest integer smaller than  $2W/\lambda_l$ , and one can verify<sup>2</sup> that in the limit  $W \gg \lambda_l$  Eq. (1) agrees with the expression for the classical Sharvin contact resistance in two dimensions. Presumably, in the experimental QPC the confining potential is smoother, but this does not affect the quantization, since Eq. (1) holds irrespective of the form of the dispersion  $\varepsilon_n(k)$ . For the same reason the quantization is retained in a magnetic field  $B$ , which has only the effect of reducing  $N$  from  $2W/\lambda_l$  to  $\pi l_{\text{cycl}}/\lambda_l = k_l l_{\text{cycl}}/2$ , once a cyclotron orbit fits into the channel [ $l_{\text{cycl}} \equiv \hbar k_l / eB$  is the cyclotron radius at the Fermi energy, with  $k_l \equiv 2\pi/\lambda_l$  the Fermi wave vector and  $B$  the magnetic field.] This is indeed observed experimentally<sup>2,3</sup>. The well-developed plateaus at zero magnetic field demonstrate experimentally that the narrow and short constriction which forms the QPC behaves very much as an ideal electron wave guide. This is surprising, and is currently being investigated theoretically<sup>14</sup>. Deviations from the ideal behavior described by Eq. (1) occur if electrons which enter the channel have a non-zero possibility  $r$  to scatter back into the broad region. This reduces  $G_c$  by a factor  $(1-r)$ . The zero-field

quantization is therefore much less robust than the quantum Hall effect, and is not likely to provide an alternative resistance standard. The point is, as emphasized by Büttiker<sup>15</sup>, that a large magnetic field suppresses back-scattering by spatially separating left- and right-moving electrons at opposite edges of the channel. One further distinction from the quantum Hall effect is that, in principle, Eq. (1) is not restricted to two dimensions, but also holds for a 3D wire with transverse dimensions of order  $\lambda_F$ .

The contact conductance  $G_c$  given by Eq. (1) refers to a two-terminal measurement,  $G_c \equiv I/e\Delta\mu$ , where the chemical potential difference  $\Delta\mu$  is measured between the source and drain for the current  $I$  (Fig. 1, inset). This quantity does not contain information on the spatial distribution of the voltage drop. Such information can be obtained from the four-terminal resistance  $R_{4t} \equiv e(\mu_L - \mu_R)/I$ , defined in terms of the chemical potentials  $\mu_L$  and  $\mu_R$  measured by two voltage probes at opposite sides of the constriction (Fig. 2, inset). Measurements<sup>16</sup> of  $R_{4t}$  have found a negative magnetoresistance which (as shown in Fig. 2) is well described by the Landauer-type formula<sup>16</sup>

$$R_{4t} = \frac{h}{2e^2} \left( \frac{1}{N} - \frac{1}{N_L} \right), \quad (2)$$

where  $N_L = k_F l_{\text{cycl}}/2$  is the number of occupied Landau levels in the broad regions adjacent to the constriction, which itself has  $N$  occupied subbands. [A similar formula has independently been obtained by Büttiker<sup>15</sup>.] The negative magnetoresistance predicted by Eq. (2) results from reduced back-scattering at the entrance of the constriction. As indicated schematically in Fig. 2 (inset), right- and left-moving electrons in the broad regions are spatially separated by a magnetic field. This reduces the probability that electrons approaching the constriction are scattered back into the broad regions, and leads to a decrease of  $R_{4t}$  with increasing  $B$ , until  $2l_{\text{cycl}} \lesssim W$ . Then  $N = N_L$  so that  $R_{4t} = 0$ , as if the constriction were not there. The two-terminal resistance  $1/G_c$  (Eq. (1)) does not vanish, of course, but becomes identical to the Hall resistance  $R_H$ ,

$$R_H = \frac{h}{2e^2} \frac{1}{N_L}. \quad (3)$$

[Note that, in the experiment shown in Fig. 2, a reduced electron density in the constriction leads to a crossover to a positive magnetoresistance at higher fields, in accordance with Eq. (2).] One could still call  $R_H$  a contact resistance, originating at the source and drain where electrons enter or leave the 2DEG with an effective "conductive width" of order  $l_{\text{cycl}}$ . This point of view is supported by the observations<sup>2,3</sup> (Fig. 1) of a continuous transition in the two-terminal resistance from zero-field quantization to quantum Hall effect.

The special role of contact resistances was not appreciated in this field until recently. The Landauer-type formula  $G = (2e^2/h)N(1-r)$ , which implies Eq.

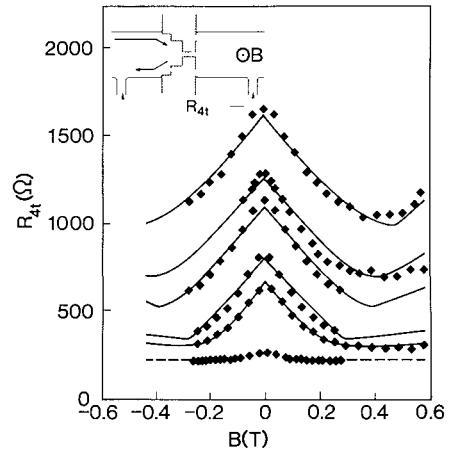


**Fig. 2.** Four-terminal magnetoconductance of a constriction for a series of gate voltages from 0 V (lowest curve) to  $-3$  V. Solid lines are according to Eq. (2), with the constriction width as adjustable parameter. The negative magnetoresistance is the result of reduced back-scattering in a magnetic field. The inset shows the device geometry. The spatial separation by a magnetic field of left- and right-moving electrons is indicated. (Fig. taken from Ref. 16.)

(1) in the absence of back-scattering ( $r = 0$ ), has long been subject to controversy – since it was not understood where the residual resistance of a perfect conductor came from<sup>17</sup>. Indeed, the original (one-dimensional) Landauer<sup>12</sup> formula  $G = (2e^2/h)(1-r)/r$  gives  $1/G = 0$  for  $r = 0$ . The question of contact resistances was settled by Imry<sup>13</sup>, just before acquiring an unexpected significance with the QPC experiments.

### 3. Quenching of the Hall effect

The familiar expression (3) for the Hall resistance is valid only in a broad 2DEG. Recent measurements<sup>6,18</sup> of  $R_H$  for ballistic transport through narrow 2DEG channels have shown deviations from Eq. (3) at sufficiently low magnetic fields. The experiments can be described in terms of two field scales. Firstly, deviations from a linear  $B$ -dependence of  $R_H$  develop below a field  $B_{\text{crit}}$ . Secondly, in the narrowest channels and at low temperatures a remarkable plateau of zero Hall resistance is found below a threshold magnetic field  $B_{\text{thres}}$ . This is the phenomenon of the quenching of the Hall effect. In Ref. 5 it was argued that these two field scales are given approximately by

$$B_{\text{crit}} \approx \frac{1}{\pi} \frac{h}{e} k_F W^{-1}, \quad (4a)$$

$$B_{\text{thres}} \approx 2 \frac{h}{e} k_F^{-1} W^{-3}. \quad (4b)$$

The field  $B_{\text{crit}}$  is reached when the channel width  $W$  is of the order of the cyclotron diameter, and the field  $B_{\text{thres}}$  when  $W$  is of the order of the transverse wave length of magnetic edge states. Good agreement was obtained with the experiments of Roukes *et al.*<sup>6</sup>, on a series of etched wires of different widths. Ford *et al.*<sup>18</sup> have recently reported significant disagreement with Eq. (4b) in a 2DEG channel of variable width, defined electrostatically by a gate potential. Uncertainties in the dependence of  $W$  and  $k_F$  on the gate potential, combined with the sensitivity of Eq. (4b) to the precise value of  $W$  (because of the  $W^{-3}$  power law), may account for part of the disagreement. Clearly further experiments on well-defined systems are necessary to settle the issue.

The arguments of Ref. 5 are based on the differences in lateral extension of states at the Fermi level, when a 2DEG channel is placed in a perpendicular magnetic field. The physics involved is conveniently discussed in terms of a "phase diagram" (Fig. 3), which illustrates the classical correspondences of the various quantum states. Classically, we can distinguish three types of trajectories in a magnetic field, depending on the energy  $\varepsilon$  (or cyclotron radius  $(2me)^{1/2}/eB$ ) and the separation  $X$  of the cyclotron orbit center from the line  $x=0$  in the middle of the channel. These are: 1. Circular cyclotron orbits, which correspond to Landau levels; 2. Skipping orbits, corresponding to edge states; and 3. Traversing trajectories, corresponding to states which interact with both boundaries. In the  $(X, \varepsilon)$  space the different types of trajectories are separated by two parabolas (Fig. 3). The quantum mechanical dispersion law  $\varepsilon_n(k)$  can be drawn into this classical "phase diagram", because of the correspondence  $k = -X eB/\hbar$ . [ This correspondence exists because both  $k$  and  $X$  are constants of the motion, and follows from the fact that the canonical momentum  $\hbar k$  along the channel equals

$$\hbar k = mv_y - eA_y = mv_y - eBx = -eBX,$$

in the Landau gauge  $\mathbf{A} = (0, Bx, 0)$ . ] We have done this in Fig. 4 for values of  $B$ ,  $W$ , and  $k_F$  (taken from Ref. 6) in each of the three regimes  $B > B_{\text{crit}}$ ,  $B_{\text{thres}} < B < B_{\text{crit}}$ , and  $B < B_{\text{thres}}$ .

If  $B > B_{\text{crit}}$  (Fig. 4a) there are no states at the Fermi level which interact with both the opposite edges of the channel. Consequently, the Hall resistance takes its normal value (Eq. (3)) for a broad 2DEG. If  $B_{\text{thres}} < B < B_{\text{crit}}$  (Fig. 4b) there are, in addition to edge states on each of the boundaries, also states at the Fermi level which interact with both edges. In this regime classical size effects lead to deviations from Eq. (3). Finally, if  $B < B_{\text{thres}}$  (Fig. 4c) there are at the Fermi level only states which interact with both edges. All edge states are suppressed, since their transverse wave length exceeds the channel width. As argued in Ref. 5, this suppression of edge states could lead to a vanishing Hall resistance. The argument is based on Büttiker's<sup>9</sup> four-terminal resistance formula, which relates resistances to transmission probabilities into voltage probes. This formula implies a vanishing Hall resistance if an

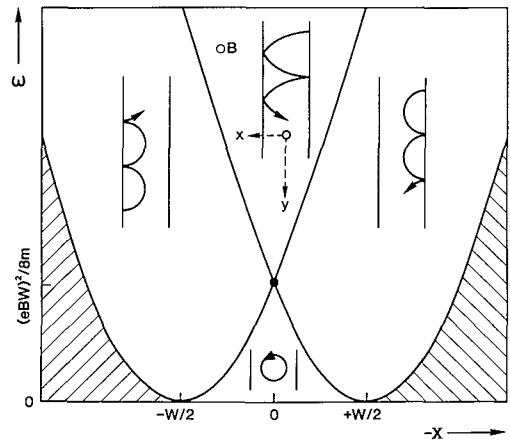
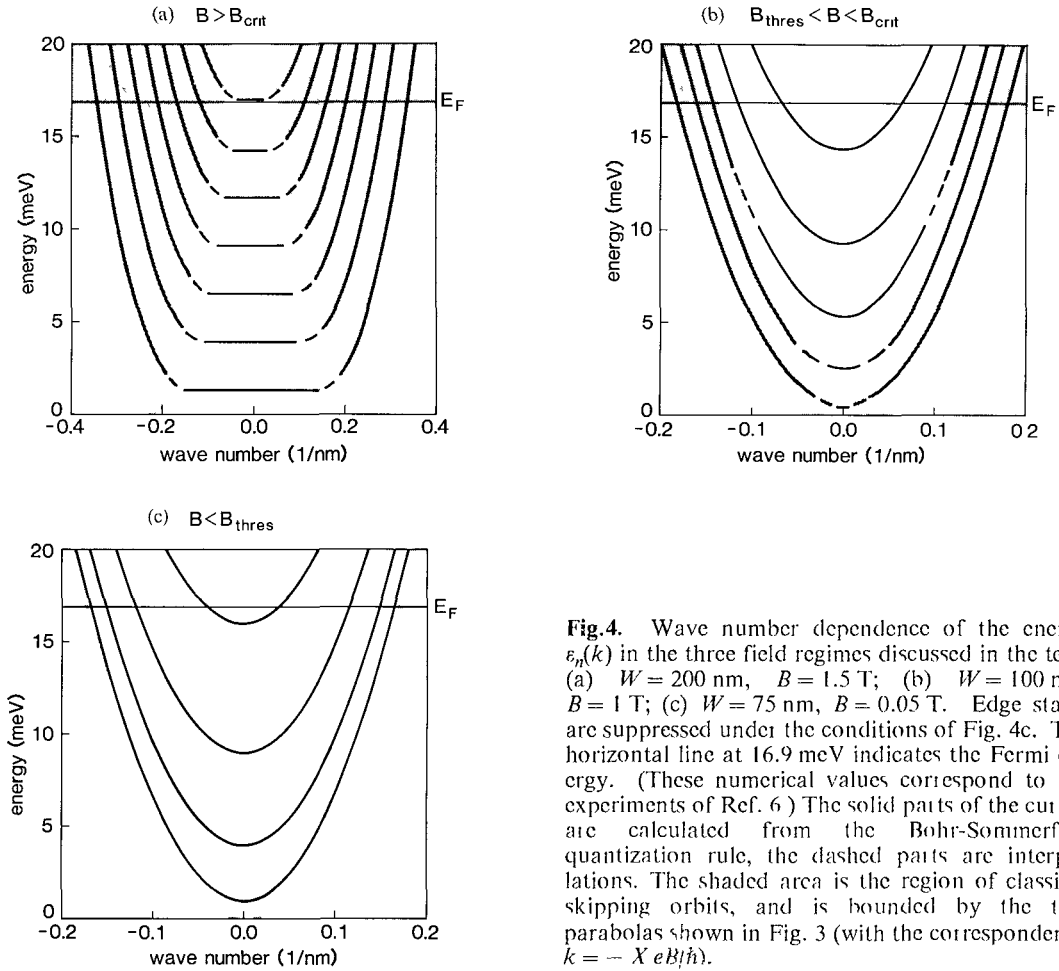


Fig.3. Energy – orbit center phase space. The two parabolas divide the space into four regions which correspond to different types of classical trajectories in a magnetic field (clockwise from left: skipping orbits on one edge, traversing trajectories, skipping orbits on the other edge, and cyclotron orbits). The shaded area is forbidden. The region at the upper center contains traversing trajectories moving in both directions, but only one direction is shown for clarity.

electron moving along the 2DEG channel has equal probability of entering one or the other of two opposite voltage probes. Since traversing trajectories collide with equal frequency on both channel boundaries, they do not contribute to the Hall voltage, so that skipping orbits are a classical prerequisite for a non-zero  $R_H$ . The classical correspondence then suggests a quenching of the Hall effect once all edge states are suppressed. A decisive test of this argument<sup>5</sup> would be a numerical calculation of the transmission probabilities in a magnetic field. This has not yet been done. Peeters<sup>19</sup> has shown that no quenching occurs if the voltage probes are weakly coupled by tunnel junctions to a conducting channel (this case can be solved analytically). The experiments are, however, performed in the opposite limit of strong coupling, where an electron has a large probability of being diverted into one of the voltage probes<sup>20</sup>. The negative result of Ref. 19 is therefore by itself not in conflict with the experiments, nor with Ref. 5 (where coupling to the voltage probes via ballistic motion, rather than tunneling, is assumed).

#### 4. Coherent electron focusing

Skipping orbits can be directly observed by means of the technique of electron focusing, pioneered in metals by Sharvin<sup>1</sup> and Tsui<sup>21</sup>. In metals, electron focusing is essentially a classical phenomenon, consisting of the focusing by a magnetic field of electrons from one point contact (injector) onto a second point contact (collector). Both point contacts are located on the same boundary, so that the classical motion from



**Fig.4.** Wave number dependence of the energy  $\epsilon_n(k)$  in the three field regimes discussed in the text. (a)  $W = 200$  nm,  $B = 1.5$  T; (b)  $W = 100$  nm,  $B = 1$  T; (c)  $W = 75$  nm,  $B = 0.05$  T. Edge states are suppressed under the conditions of Fig. 4c. The horizontal line at 16.9 meV indicates the Fermi energy. (These numerical values correspond to the experiments of Ref. 6) The solid parts of the curves are calculated from the Bohr-Sommerfeld quantization rule, the dashed parts are interpolations. The shaded area is the region of classical skipping orbits, and is bounded by the two parabolas shown in Fig. 3 (with the correspondence  $k = -X e B / \hbar$ ).

injector to collector consists of skipping orbits (for a specularly reflecting boundary). Focusing occurs if the point contact separation  $L$  is an integer multiple of the cyclotron diameter, that is for fields  $B$  which are multiples of

$$B_{\text{focus}} = 2 \frac{\hbar k_F}{eL} \quad (5)$$

The classical focusing spectrum consists of a series of peaks in the collector voltage of equal height and constant separation  $B_{\text{focus}}$ . Such a spectrum is commonly observed in metals<sup>22</sup>, albeit with a decreasing height of subsequent peaks because of partially diffuse scattering.

The electron focusing spectrum in a 2DEG, reported in Ref. 7, is strikingly different. At low fields a series of focusing peaks is, indeed, observed at the expected positions — demonstrating specular reflection at the mirror formed by the gate potential. However, finestructure is superimposed on the focusing peaks at low temperatures. Moreover, at higher fields the collector voltage shows oscillations with a

much larger amplitude than the low-field focusing peaks, although retaining  $B_{\text{focus}}$  as the dominant periodicity. As we have shown in Ref. 8, the interference at the collector of different phase coherent skipping orbits can explain the essential features of the experiments. The difference between coherent and classical electron focusing is one of length scales: The ratios  $\lambda_F/W$  and  $\lambda_F/L$  are, respectively,  $10^2$  and  $10^4$  times larger in the 2DEG than in a typical metal! The significance of CEF is that it demonstrates that an interference experiment can be realized with a QPC as point source and detector.

In this section we would like to discuss CEF from a different point of view, as a typical example of a non-local voltage measurement<sup>23</sup>. The injector is the current source, and the collector a voltage probe. The non-locality of the voltage measurement manifests itself in the dependence of the collector voltage  $V_c$  on the point contact separation  $L$ . In the geometry shown in the inset of Fig. 5, the focusing peaks appear in one field direction as modulations of the normal Hall voltage. The non-local Hall resistance  $V_c/I_i$  shown in

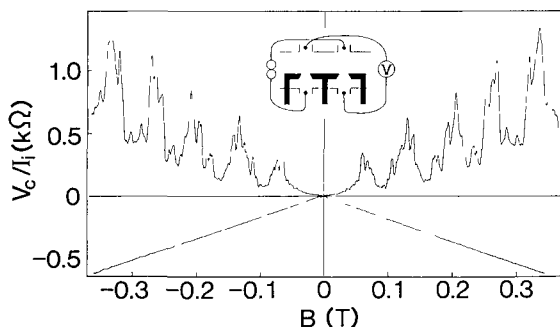


**Fig.5.** Electron focusing spectrum showing focusing peaks at multiples of  $B_{\text{focus}} \approx 0.066$  T (Eq. (5) with  $k_F = 1.5 \times 10^8 \text{ m}^{-1}$  and  $L = 3.0 \mu\text{m}$ ). Note the interference fringes. For reverse fields the normal Hall resistance is seen. The inset gives the experimental configuration, with the gate defining the injector and collector point contacts and the 2DEG boundary shown in black. The two experimental traces correspond to interchanged current and voltage leads, and demonstrate the injector-collector reciprocity. (Fig. taken from Ref. 23.)

Fig. 5 (with  $I_i$  the injected current) is alternately smaller and larger than its normal value (Eq. (3)) which is observed in reverse fields. [Note the fine structure on the focusing peaks; The large high-field oscillations mentioned above are outside the range of this figure.] Fig. 5 contains two experimental traces (one with focusing peaks for positive  $B$  and one for negative  $B$ ), which were obtained upon interchanging current and voltage leads — so that the injector becomes the collector and *vice versa*. The reciprocity of injector and collector is evident and is in agreement with the reciprocity relation for four-terminal phase coherent conductances which was recently derived by Büttiker<sup>9</sup>. This nicely demonstrates the validity of symmetries of the Onsager-Casimir type in non-local voltage measurements (see Ref. 20 for other experimental confirmations).

**Acknowledgement-** This article is based on work done in collaboration with H. Ahmed, M.E.I. Broekaart, C.T. Foxon, J.J. Harris, L.P. Kouwenhoven, P.H.M. van Loosdrecht, D. van der Marel, J.E. Mooij, M. Pepper, T.J. Thornton, and J.G. Williamson. We thank J.A. Pals and M.F.H. Schuurmans for support.

### References

1. Yu.V. Sharvin, *Soviet Physics JETP* **21**, 655 (1965). For a review, see A.G.M. Jansen, A.P. van Gelder, and P. Wyder, *Journal of Physics C* **13**, 6073 (1980).
2. B.J. van Wees, H. van Houten, C.W.J. Beenakker, J.G. Williamson, L.P. Kouwenhoven, D. van der Marel, and C.T. Foxon, *Physical Review Letters* **60**, 848 (1988); B.J. van Wees, *et al.*, *Physical Review B* (to be published).
3. D.A. Wharam, T.J. Thornton, R. Newbury, M. Pepper, H. Ahmed, J.E.F. Frost, D.G. Hasko, D.C. Peacock, D.A. Ritchie, and G.A.C. Jones, *Journal of Physics C* **21**, L209 (1988).
4. G. Timp, A.M. Chang, P. Mankiewich, R. Behringer, J.E. Cunningham, T.Y. Chang, and R.E. Howard, *Physical Review Letters* **59**, 732 (1987).
5. C.W.J. Beenakker and H. van Houten, *Physical Review Letters* **60**, 2406 (1988).
6. M.L. Roukes, A. Scherer, S.J. Allen, Jr., H.G. Craighead, R.M. Ruthen, E.D. Beebe, and J.P. Harbison, *Physical Review Letters* **59**, 3011 (1987).
7. H. van Houten, B.J. van Wees, J.E. Mooij, C.W.J. Beenakker, J.G. Williamson, and C.T. Foxon, *Europhysics Letters* **5**, 721 (1988).
8. C.W.J. Beenakker, H. van Houten, and B.J. van Wees, *Europhysics Letters* (to be published).
9. M. Büttiker, *Physical Review Letters* **57**, 1761 (1986); *IBM Journal of Research and Development* **32**, 317 (1988).
10. T.P. Smith, III, J.A. Brum, J.M. Hong, C.M. Knoedler, H. Arnot, and L. Esaki (preprint).
11. Alternative explanations have been given by D.A. Wharam *et al.* (Ref. 3), by Y. Isawa (preprint), and by R. Johnston and L. Schweitzer (preprint).
12. R. Landauer, *IBM Journal of Research and Development* **1**, 223 (1957); **32**, 306 (1988); *Zeitschrift für Physik B* **68**, 217 (1987).
13. Y. Imry, in *Directions in Condensed Matter Physics*, Vol. 1, edited by G. Grinstein and G. Mazenko (World Scientific, Singapore, 1986) page 129.
14. E.G. Haanappel and D. van der Marel (preprint); A.D. Stone and A. Szafer (private communication).
15. M. Büttiker (preprint).
16. H. van Houten, C.W.J. Beenakker, P.H.M. van Loosdrecht, T.J. Thornton, H. Ahmed, M. Pepper, C.T. Foxon, and J.J. Harris, *Physical Review B* **37**, 8534 (1988).
17. A discussion of this controversy is given by A.D. Stone and A. Szafer, *IBM Journal of Research and Development* **32**, 384 (1988).
18. C.J.B. Ford, T.J. Thornton, R. Newbury, M. Pepper, H. Ahmed, D.C. Peacock, D.A. Ritchie, J.E.F. Frost, and G.A.C. Jones (preprint).
19. F.M. Peeters, *Physical Review Letters* **61**, 589 (1988).
20. A.D. Benoit, S. Washburn, C.P. Umbach, R.B. Laibowitz, and R.A. Webb, *Physical Review Letters* **57**, 1765 (1986); G. Timp, H.U. Baranger, P. deVegvar, J.E. Cunningham, R.E. Howard, R. Behringer, and P.M. Mankiewich, *Physical Review Letters* **60**, 2081 (1988).
21. V.S. Tsui, *JETP Letters* **19**, 70 (1974).
22. P.A.M. Benistant, G.F.A. van de Walle, H. van Kempen, and P. Wyder, *Physical Review B* **33**, 690 (1986).
23. H. van Houten, C.W.J. Beenakker, J.G. Williamson, M.E.I. Broekaart, P.H.M. van Loosdrecht, B.J. van Wees, J.E. Mooij, C.T. Foxon, and J.J. Harris, to be published.